



ELSEVIER

International Journal of Mass Spectrometry 185/186/187 (1999) 449–462



Competitive elimination of methane and ethylene from trimethylsilyl-substituted silylenium ions

Belinda B. Willard, Susan T. Graul*

Department of Chemistry, Carnegie Mellon University, Pittsburgh, PA 15213, USA

Received 5 June 1998; accepted 19 November 1998

Abstract

Metastable dissociations have been studied for trimethylsilyldimethylsilylenium ion, $(\text{CH}_3)_3\text{Si}-\text{Si}^+(\text{CH}_3)_2$, and four bridged analogs, $(\text{CH}_3)_3\text{Si}-\text{X}-\text{Si}^+(\text{CH}_3)_2$ ($\text{X} = \text{CH}_2, \text{O}, \text{NH}, \text{C}\equiv\text{C}$). Several dissociation pathways are observed, with branching ratios that vary significantly with the bridging group. This article focuses on two competing pathways: elimination of methane and of ethylene. The energetics of ethylene elimination from $(\text{CH}_3)_3\text{Si}-\text{Si}^+(\text{CH}_3)_2$ have been characterized by molecular orbital and density functional theory, and the kinetic energy distributions of the products of the dissociation have been modeled with statistical phase space theory, yielding good agreement with experiment. Methane elimination occurs across the two silicon centers, and is accompanied by a large release of kinetic energy, suggestive of a concerted reaction and a considerable reverse activation barrier in the exit channel. Electronic structure calculations combined with statistical phase space modeling of the dissociation kinetics suggest that the product from methane elimination is a disilacyclobutyl cation. A mechanism for this elimination reaction is proposed. A comparison of the kinetic energy release distributions observed for methane elimination from the bridged ions suggests that an analogous mechanism is involved for the entire series. (Int J Mass Spectrom 185/186/187 (1999) 449–462) © 1999 Elsevier Science B.V.

Keywords: Organosilicon; Metastable dissociation; Theory; Unimolecular reaction

1. Introduction

One of our research interests is finding experimental and theoretical means to characterize the mechanisms of reactions of ions in the gas phase, with particular emphasis on reactions of fundamental interest for organic chemistry, such as nucleophilic substitution reactions, oxidations, and elimination reactions. During the past few years, we have been studying the metastable

dissociations of organosilicon ions, specifically of silylenium ions **I**, the silicon analogs of carbenium ions. These species share some of the characteristics of carbenium ions, such as a tendency to undergo facile rearrangements [1–9]. However, because there are often large differences in energies for the isomeric silylenium and carbenium ions derived from, for example, 1,2-atom or -group shifts, barriers to rearrangements tend to be larger in silylenium ions [10–12], leading to the possibility of distinguishing isomeric species by collisional activation or reactivity studies [13–16]. In a recent study, we showed that kinetic energy analysis of the product ions from metastable dissociation of isomeric SiC_2H_7^+ (i.e.

* Corresponding author.

Dedicated to Professor Mike Bowers on the occasion of his 60th birthday.

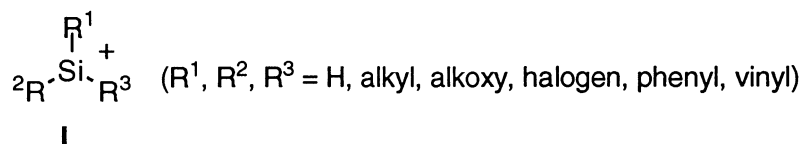


Diagram 1.

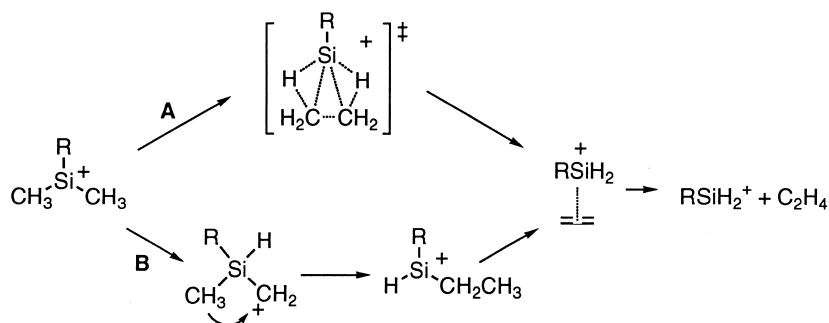
$\text{HSi}^+(\text{CH}_3)_2$ and $\text{H}_2\text{Si}^+\text{C}_2\text{H}_5$) and SiC_3H_9^+ [as $(\text{CH}_3)_3\text{Si}^+$ and $\text{HSi}^+(\text{CH}_3)(\text{C}_2\text{H}_5)$ isomers] silylenium ions could be used along with theoretical modeling to gain insight to the mechanisms of rearrangements [17]. These particular systems were of interest because they had been reasonably thoroughly characterized in earlier studies and were also fairly simple molecules, and therefore could provide a theoretically accessible benchmark for the metastable analysis. Numerous other silylenium ions with larger alkyl substituents, heteroatom substituents, and unsaturation have also been studied and some of those results will be described in future publications.

Here, we describe results from studies of five trimethylsilyl-substituted silylenium ions: $(\text{CH}_3)_3\text{Si-Si}^+(\text{CH}_3)_2$ and $(\text{CH}_3)_3\text{Si-X-Si}^+(\text{CH}_3)_2$ ($\text{X} = \text{CH}_2, \text{NH}, \text{O}$, and $\text{C}\equiv\text{C}$). These systems stood out from the rest in that they all exhibit, to varying degrees, a metastable dissociation pathway that has not been observed for any monosilicon silylenium ion we have studied thus far. In addition to the ethylene elimination reaction also observed for the SiC_2H_7^+ and SiC_3H_9^+ ions and several other dimethyl-substituted silylenium ions, the trimethylsilyl-substituted silylenium ions also dissociated by loss of methane [18]. We have examined this process along with the ethylene elimination pathway, by means of mass-analyzed ion kinetic energy spectroscopy (MIKES), combined with electronic structure calculations for determination of reaction energetics, and statistical phase space theoretical modeling of the kinetic energy release associated with the metastable reactions. The results indicate that the ionic product of methane elimination is a methylated disilacyclobutyl cation.

2. Experiment

Experiments were performed using a reverse geometry double focusing mass spectrometer (V. G. Analytical ZAB-IF). The ions were generated by

dissociative electron ionization (50 or 70 eV) at low source pressures. Although direct source pressure measurement is not currently available in this instrument, the source conditions are known to be essentially collisionless, in that no products of expected ion-molecule chemistry are observed under typical operating conditions. Ions were extracted from the source, accelerated to 8 keV, and the ion of interest mass selected at the magnetic sector. Products of metastable dissociations in the field free region between the magnet and electric sectors were energy analyzed by scanning the electrostatic sector, a technique known as MIKES. Dissociations occurring in this region correspond to lifetimes of approximately 10 μs . Branching ratios were obtained by integrating each product ion peak area. The kinetic energy release distributions (KERDs) were obtained from analysis of the peak shape by one of two procedures. For narrow peaks (average release less than 0.2 eV), the KERD is obtained from numerical differentiation of the peak shape and transformation of coordinates, a method that has been described previously [19]. This method neglects instrumental discrimination and assumes a point source of dissociation, and can overestimate energy releases for broad peaks (average release greater than 0.5 eV). For such peaks, instrumental discrimination can lead to significant distortion of the peak shape, and a more sophisticated method was used to obtain the KERDs. This method is based on the work of Rumpf and Derrick [20], and involves calculation of several "basis functions" corresponding to peak shapes for single-valued energy releases. The calculation accounts for instrumental discrimination and for dissociation throughout the field-free region. The basis functions are collected into a rectangular matrix, and a fit to the data is obtained by means of singular value decomposition. This procedure allows for editing of the resulting matrix of singular values,



Scheme 1. Mechanisms for elimination of ethylene from dimethyl silylenium ions.

thereby eliminating solutions that do not contribute significantly to improving the fit. The more straightforward procedure of least-squares fitting can result in large oscillations in the resulting KERD, because of addition and subtraction of linear combinations of basis functions that serve mainly to fit noise.

Hexamethyldisilane, hexamethyldisiloxane, hexamethyldisilazane, bis(trimethylsilyl)methane, bis(trimethylsilyl)acetylene, and 1,1,2,2-tetrachloro-1,2-dimethyldisilane were purchased from Sigma-Aldrich. 1,2-dichloro-1,2-dimethyl-1,2-diphenyldisiloxane was obtained from Gelest Inc., PA. All compounds were used without further purification.

Ab initio calculations were performed using the GAUSSIAN 92 [21] and GAUSSIAN 94 [22] software packages, running on a DEC alpha server (model 400). All geometries were optimized using the 6-31G(*d,p*) basis set at the Hartree-Fock (HF) level of theory. Frequencies were calculated at the HF level and were corrected by a factor of 0.893 [23]. For the purpose of comparison, these calculations were also carried out using density functional theory at the Becke3LYP/6-31G(*d*) level.

Theoretical modeling of the KERDs was performed using statistical phase space theory [24–27]. These calculations are described briefly in an Appendix.

3. Results and discussion

Our studies of a number of dimethyl- or ethyl-substituted silylenium ions have shown that a common and often prominent metastable dissociation

pathway is elimination of ethylene. For dimethyl-substituted ions, the elimination can occur by two different mechanisms that both lead to a common intermediate, a silylenium-bridged ethylene (Scheme 1) [10–12]. One mechanism involves isomerization to the ethyl-substituted isomer by way of the α -silyl carbenium ion. The ethyl-substituted ion then rearranges to the bridged structure by either β -hydrogen transfer or sequential 1,2-hydrogen shifts. The alternative mechanism involves a cyclic transition state with concerted carbon–carbon bond formation and transfer of two hydrogens to the silicon atom. The theoretical barriers for these two processes were found to be comparable at the MP2/6-31G(*d,p*) level of theory [17].

The metastable dissociation spectrum of $(\text{CH}_3)_3\text{Si-Si}^+(\text{CH}_3)_2$ revealed an intriguing difference from other dimethyl-substituted silylenium ions. Elimination of ethylene was only a very minor pathway, and a new dissociation channel was observed, corresponding to elimination of methane. This pathway has not been observed by us for metastable dissociations of any silylenium ions that contain only a single silicon center, but is observed in each of the trimethylsilyl-substituted silylenium ions that we have studied, and has been reported in the literature for $(\text{CH}_3)_3\text{Si-NH-Si}^+(\text{CH}_3)_2$ and $(\text{CH}_3)_3\text{Si-O-Si}^+(\text{CH}_3)_2$ [18,28] and for ions from trimethylsilyl-substituted chlorosilanes [29]. The branching ratios for the metastable dissociations of $(\text{CH}_3)_3\text{Si-Si}^+(\text{CH}_3)_2$ and $(\text{CH}_3)_3\text{Si-X-Si}^+(\text{CH}_3)_2$ ($\text{X} = \text{CH}_2, \text{NH}, \text{O}, \text{C}\equiv\text{C}$) are given in Table 1. It can be seen that methane elimination

Table 1

Experimental branching ratios for the metastable decomposition of $(\text{CH}_3)_3\text{Si-Si}^+(\text{CH}_3)_2$ and $(\text{CH}_3)_3\text{Si-X-Si}^+(\text{CH}_3)_2$ ions ($\text{X} = \text{CH}_2, \text{NH}, \text{O}, \text{C}\equiv\text{C}$)

Ion	Neutral loss	Percent abundance ^a
$(\text{CH}_3)_3\text{Si-Si}^+(\text{CH}_3)_2$	$\text{Si}(\text{CH}_3)_2$	47
	H_2	35
	CH_4	12
	C_2H_4	6
$(\text{CH}_3)_3\text{Si-CH}_2\text{-Si}^+(\text{CH}_3)_2$	CH_4	60
	$\text{CH}_2\text{Si}(\text{CH}_3)_2$	29
	C_2H_4	8
	$\text{H}_2\text{Si}(\text{CH}_3)_2$	3
$(\text{CH}_3)_3\text{Si-NH-Si}^+(\text{CH}_3)_2$	CH_4	>99
	$\text{NHSi}(\text{CH}_3)_2$	<1
$(\text{CH}_3)_3\text{Si-O-Si}^+(\text{CH}_3)_2$	CH_4	80
	$\text{OSi}(\text{CH}_3)_2$	16
	C_2H_4	4
$(\text{CH}_3)_3\text{Si-C}\equiv\text{C-Si}^+(\text{CH}_3)_2$	C_2H_4	23
	C_2H_2	20
	$\text{Si}(\text{CH}_3)_2$	18
	SiC_4H_6	13
	$\text{H}_2\text{Si}(\text{CH}_3)_2$	10
	C_3H_4	7
	CH_4	6
C_3H_6	3	

^a Integrated product intensity. Typical reproducibility is $\pm 1\text{--}2\%$.

dominates for three of the ions: Those with $\text{X} = \text{CH}_2, \text{NH}$, and O . It is less prominent for $(\text{CH}_3)_3\text{Si-}$

$\text{Si}^+(\text{CH}_3)_2$ and for $\text{X} = \text{C}\equiv\text{C}$. Formation of a product ion corresponding to $(\text{CH}_3)_3\text{Si}^+$ is common to all five ions (although it is only a trace product for $\text{X} = \text{NH}$). The $\text{C}\equiv\text{C}$ -bridged ion gives numerous products, suggesting that extensive rearrangement is occurring. The variation in the extent of methane elimination for these five ions is significant, ranging from >99% for $\text{X} = \text{NH}$ to only 6% for $\text{X} = \text{C}\equiv\text{C}$. Loss of ethylene, by contrast, was a minor pathway, except in the $\text{C}\equiv\text{C}$ -bridged ion.

The shapes of the KERDs for C_2H_4 and CH_4 loss from these ions give some insight into the mechanisms involved [30]. The experimental KERDs for C_2H_4 and CH_4 elimination from $(\text{CH}_3)_3\text{Si-Si}^+(\text{CH}_3)_2$ are shown in Fig. 1. Loss of C_2H_4 is accompanied by a small energy release and an energy distribution peaked near zero, suggesting a process that does not involve a reverse activation barrier (that is, an exit-channel energy barrier relative to the separated products). In contrast, the energy release for CH_4 loss is large, and the distribution is broad and peaked well away from zero. This type of KERD is indicative of a process which has a large reverse activation barrier and suggests that CH_4 loss may be a concerted process.

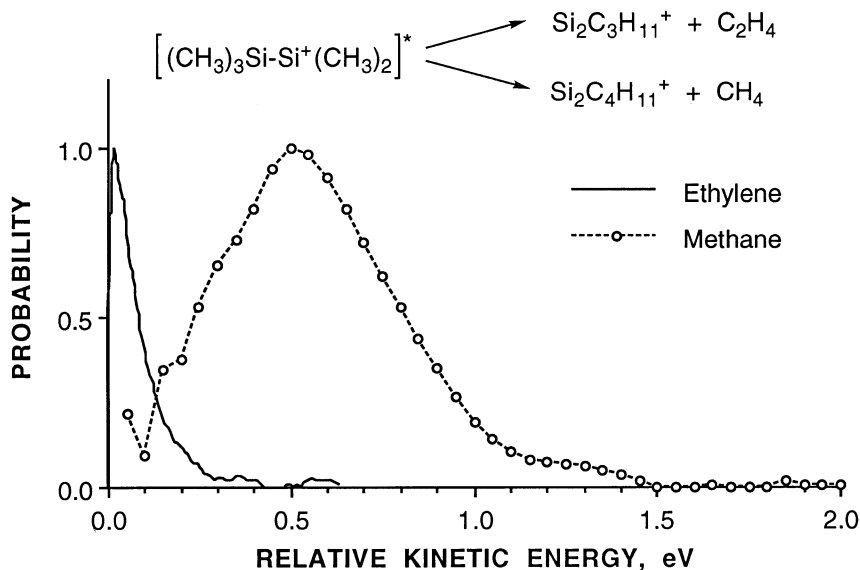
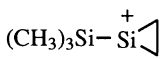
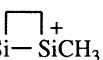
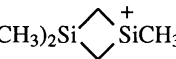
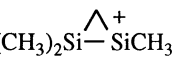
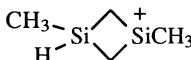


Fig. 1. Experimental kinetic energy release distributions for metastable dissociation of $(\text{CH}_3)_3\text{Si-Si}^+(\text{CH}_3)_2$.

Table 2

Reaction enthalpies at 0 K for some possible ionic products from metastable dissociation of $(\text{CH}_3)_3\text{Si}-\text{Si}^+(\text{CH}_3)_2$ ^a

Neutral Loss	Product Ion	HF/6-31G(d,p)	Becke3LYP/6-31G(d)
$(\text{CH}_3)_2\text{Si}$	$(\text{CH}_3)_3\text{Si}^+$	2.29	2.41
H_2	$(\text{CH}_3)_3\text{Si}-\text{CH}=\text{Si}^+\text{CH}_3$	3.23	2.81
	$(\text{CH}_3)_3\text{Si}-\text{CH}_2\text{Si}^+=\text{CH}_2$	3.37	2.98
	$(\text{CH}_3)_3\text{Si}-\text{Si}^+$ 	2.72	2.48
	$(\text{CH}_3)_2\text{Si}-\text{Si}^+\text{CH}_3$ 	1.76	1.53
	$(\text{CH}_3)_2\text{Si}-\text{Si}^+\text{CH}_3$ 	0.93	0.79
CH_4	$(\text{CH}_3)_2\text{Si}-\text{Si}^+\text{CH}_3$ 	1.95	1.80
	$\text{CH}_3-\text{Si}-\text{Si}^+\text{CH}_3$ 	0.82	0.80
C_2H_4	$(\text{CH}_3)_3\text{Si}-\text{Si}^+\text{H}_2$	2.25	2.49
	$(\text{CH}_3)_2(\text{H})\text{Si}-\text{Si}^+(\text{CH}_3)(\text{H})$	2.00	2.18
	$(\text{CH}_3)(\text{H})_2\text{Si}-\text{Si}^+(\text{CH}_3)_2$	1.86	

^a These energies are quoted in units of eV relative to the precursor ion, $(\text{CH}_3)_3\text{Si}-\text{Si}^+(\text{CH}_3)_2$, and have been corrected for zero-point vibrational energy.

In order to gain some insight to the structure of the product ions formed upon metastable dissociation of $(\text{CH}_3)_3\text{Si}-\text{Si}^+(\text{CH}_3)_2$, electronic structure calculations were performed to determine the energetics for formation of different ionic isomers that could result from loss of H_2 , CH_4 , or C_2H_4 . The results are collected in Table 2. The major dissociation channel results in formation of $(\text{CH}_3)_3\text{Si}^+$ and is endothermic by 2.41 eV. (Formation of the isobaric ion, $\text{HSi}^+(\text{CH}_3)(\text{C}_2\text{H}_5)$, is an additional 0.82 eV endothermic [17] and was therefore not considered). The KERD for formation of this product is narrow and peaked near zero, which indicates that the effective barrier of this dissociation with respect to the precursor is approximately equal to the overall endothermicity. For the other dissociations to compete, the barriers leading to the other three products should not be significantly greater than 2.4 eV. Even with this constraint, there are multiple isomeric structures possible for the ions resulting from each of the remaining three dissociations.

The results of the electronic structure calculations were combined with the observed experimental data for metastable dissociation to create a preliminary model of the reaction coordinate for the dissociation of $(\text{CH}_3)_3\text{Si}-\text{Si}^+(\text{CH}_3)_2$. A schematic of the model used is shown in Fig. 2. The kinetic energy releases associated with loss of $(\text{CH}_3)_2\text{Si}$ or C_2H_4 are small and the KERDs are peaked near zero, so these channels were modeled with orbiting transition states in the dissociation channel and no reverse activation barrier. The kinetic energy releases for loss of H_2 or CH_4 were large and the KERDs were indicative of significant reverse activation barriers. Therefore, tight transition states were assumed for these channels. Further details regarding the assumed spectroscopic properties of these transition states are provided in the Appendix.

With use of this model reaction coordinate, the kinetics of the dissociations were calculated with statistical phase space theory, and the relative energies of the four transition states were varied until the

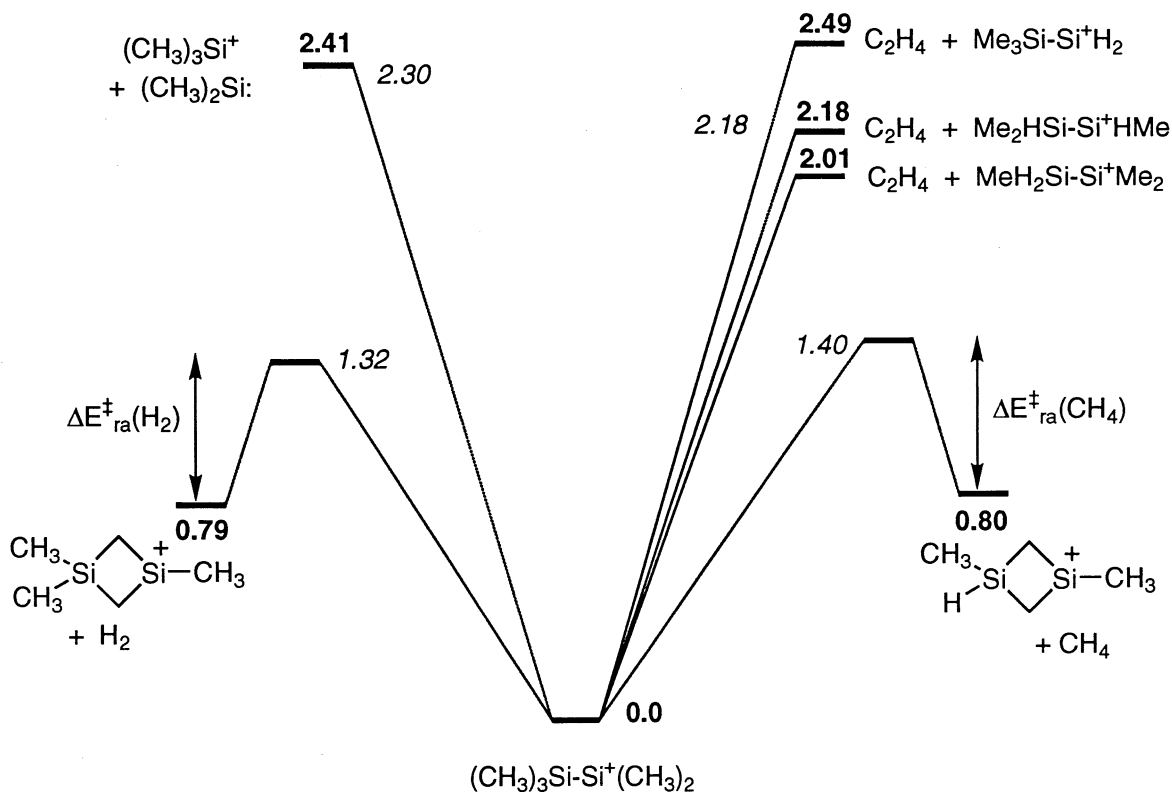


Fig. 2. Schematic drawing of the model potential energy surface used in the statistical phase space calculations for calculation of the branching ratios and the KERD for C_2H_4 loss from $(\text{CH}_3)_3\text{Si-Si}^+(\text{CH}_3)_2$. The connection of the reactant ion to the products or tight transition states may not be direct, but may involve intermediate steps, and only rate-limiting transition states are considered. All energies are given in eV and are relative to the reactant ion. Shown in bold are the 0 K enthalpies calculated at the Becke3LYP/6-31G(d) level of theory. In italics are the optimized transition state energies used in the phase space modeling of C_2H_4 loss for calculation of the KERD shown in Fig. 3. The tight transition states for H_2 or CH_4 loss represent reverse activation barriers, $\Delta E_{ra}^{\ddagger}(\text{RH})$, for these products, leading to the large releases of kinetic energy observed for these products.

experimental branching ratio was reproduced. In order to limit the scope of the problem, a constraint was imposed that the endothermicity for dissociation by loss of $(\text{CH}_3)_2\text{Si}$ must be within 0.2 eV of the theoretical result. The resulting optimized transition state energies relative to the precursor ion are given in Table 3, along with the theoretical branching ratios for these energies. It can be seen that the relative energy for the C_2H_4 dissociation channel is within the range of energies calculated for the three mostly likely isomers of the product ion, and is in excellent agreement with the B3LYP result for formation of $(\text{CH}_3)_2(\text{H})\text{Si-Si}^+(\text{CH}_3)(\text{H})$. The major factor that controls the relative amounts of $(\text{CH}_3)_2\text{Si}$ and C_2H_4

loss in the phase space calculation is the energy difference between the two orbiting transition states. When the orbiting transition state for $(\text{CH}_3)_2\text{Si}$ loss was held between 2.2 and 2.5 eV, the experimental ratio of 8 : 1 was best reproduced for an energy difference of about 0.12 eV, with the C_2H_4 loss channel being lower in energy. The calculated branching ratios for H_2 and CH_4 loss were found to be sensitive to variation in the lowest frequencies of the corresponding tight transition states, especially those frequencies below 100 cm^{-1} , so these energies have larger uncertainties associated with them. However, the modeling does show that the tight transition states must be considerably lower in energy than either of

Table 3

Optimized barrier heights from phase space theoretical modeling of the metastable dissociation of $(\text{CH}_3)_3\text{Si-Si}^+(\text{CH}_3)_2$

Neutral product	Type of transition state	Optimized barrier heights, eV ^a	Calculated branching ratio, %	Experimental branching ratio, %
$(\text{CH}_3)_2\text{Si}$	Orbiting	2.30 ± 0.15^b	48	47
H_2	Tight	1.32 ± 0.20^c	34	35
CH_4	Tight	1.40 ± 0.20^c	11	12
C_2H_4	Orbiting	2.18 ± 0.15^b	6	6

^a Energy relative to the precursor ion.^b Constrained to be within 0.2 eV of ab initio results; the uncertainty represents the range explored.^c Uncertainty represents effect of varying lowest vibrational frequencies.

the orbiting transition states in order to reproduce the experimental branching ratios. This has important implications for determining the likely structures of the product ions, and we will consider these channels next.

The metastable eliminations of H_2 or CH_4 from $(\text{CH}_3)_3\text{Si-Si}^+(\text{CH}_3)_2$ are accompanied by large releases of kinetic energy. In the case of CH_4 loss, the average kinetic energy release is about 0.5 eV, and for H_2 loss, the average release is about 0.7 eV. The shapes of the KERDs in both cases are roughly triangular, centered about the average energy. This shape is characteristic of dissociation from a repulsive potential energy surface, for example, from an acti-

vation barrier in the exit channel. To a rough approximation, the average kinetic energies for these processes may be taken as a measure of the barrier height relative to the separated products, $\Delta E_{\text{tra}}^\ddagger$ in Fig. 2. This means that the energies of the products from elimination of CH_4 should be about 0.9 eV relative to the precursor, and the products from H_2 loss should lie about 0.6 eV above the precursor ion, $(\text{CH}_3)_3\text{Si-Si}^+(\text{CH}_3)_2$. This rules out all the isomeric structures considered for these two products except the lowest energy species for each, the 1,3-disilacyclobutyl cations (Table 2).

With use of the model shown in Fig. 3 and the transition state energies in Table 3, the statistical

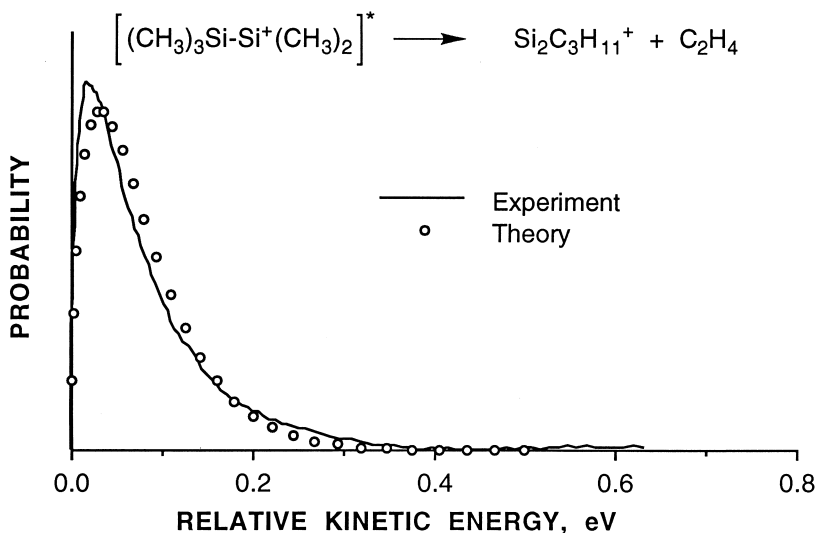
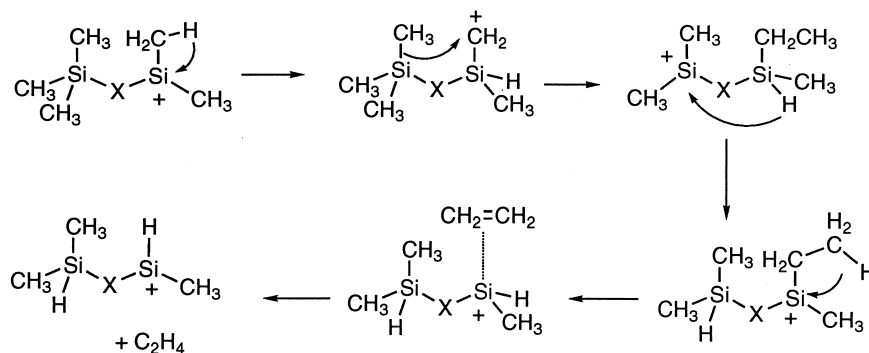


Fig. 3. Comparison of the experimental and phase space theoretical KERD for elimination of C_2H_4 from $(\text{CH}_3)_3\text{Si-Si}^+(\text{CH}_3)_2$. The theoretical KERD was calculated using the potential energy surface shown in Fig. 2 with the energies shown in italics for the rate-limiting steps in the four reaction channels.



Scheme 2. Stepwise elimination of ethylene across the silicon centers.

KERD for ethylene elimination was calculated and is compared with the experimental result in Fig. 3. For this calculation, the transition state energies were again varied over the ranges given in Table 3, with the requirement that the experimental branching ratios be reproduced. The theoretical result shown was calculated with the transition state energies shown in italics in Fig. 2. The theoretical and experimental KERDs are in good agreement, and the transition state energies are consistent with the calculated energetics of the lowest energy products for all but the C_2H_4 elimination reaction. The branching ratios can also be reproduced if each transition state energy is raised proportionately, and then the resulting theoretical KERD broadens. For example, the KERD calculated with ΔE for C_2H_4 loss at 2.29 eV has an average kinetic energy of 82 meV, compared with 78 meV when ΔE for C_2H_4 loss is 2.18 eV. Likewise, if the transition state energies are lowered proportionately, the calculated KERD narrows. However, for energies within 0.2 eV of the ab initio results, the agreement between theory and experiment is quite good.

Elimination of ethylene from $(CH_3)_3Si-Si^+(CH_3)_2$ may occur by a mechanism analogous to that shown in Scheme 1 for the dimethylated monosilicon ions, which would lead to the $(CH_3)_3Si-Si^+H_2$ product, the highest energy isomer shown for this channel in Table 2. However, studies of the dissociations of partially deuterated $(CD_3)_3Si-O-Si^+(CH_3)_2$ showed that 1,3-transfers of the methyl groups across the bridging atom are facile, leading to complete scrambling of the

labeled methyl groups [18]. This suggests that elimination of ethylene can also occur across the silicon centers (Scheme 2), which would lead to $(CH_3)_2(H)Si-Si^+(CH_3)(H)$. Formation of the lowest energy isomer for ethylene elimination in Table 2 would appear to involve a charge-remote mechanism, with the ethylene fragment deriving solely from the uncharged silicon center. We cannot distinguish among these options based on the energetics, but the similarity of the experimental KERD to that observed for monosilicon ions suggests that the charged center is involved.

Experimental kinetic energy release distributions for C_2H_4 loss from the series of $(CH_3)_3Si-X-Si^+(CH_3)_2$ ions are shown in Fig. 4. The KERD for the $X = CH_2$ ion is the same width as that for $(CH_3)_3Si-Si^+(CH_3)_2$. For $X = O$ and $C\equiv C$, the KERDs are slightly broader. The similarity in shape of the KERDs suggests that the mechanisms for ethylene loss in all four systems are very similar. The slightly greater energy release for the $X = O$ and $X = C\equiv C$ distributions may be because of the increased endothermicity for the reactions (Table 4). Stabilization of the silylenium ion in these two species can occur by π -electron donation with $X = O$ bridge and by conjugation of the positive charge into the acetylene bridge for $X = C\equiv C$, leading to the increased endothermicity. There may also be differences in the extent to which ethylene is lost by the mechanism shown in Scheme 1 versus Scheme 2, because of the steric requirements of the methyl

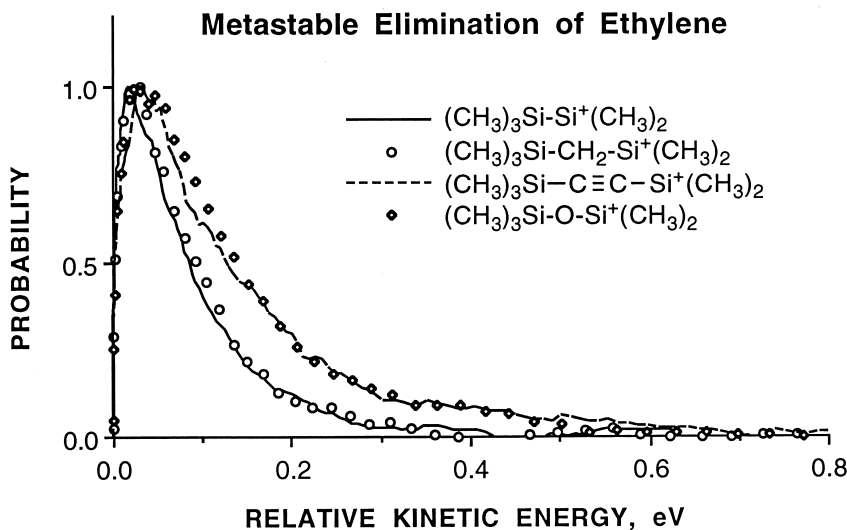


Fig. 4. Comparison of the experimental kinetic energy release distributions in $(\text{CH}_3)_3\text{Si-Si}^+(\text{CH}_3)_2$ and the $(\text{CH}_3)_3\text{Si-X-Si}^+(\text{CH}_3)_2$ series ($X = \text{CH}_2, \text{C}\equiv\text{C}, \text{O}$). This reaction channel is not observed for $X = \text{NH}$.

transfers across the bridging group, particularly for $X = \text{C}\equiv\text{C}$.

As noted above, we have not observed elimination of CH_4 metastable dissociations of the monosilicon silylenium ions. Tabei et al. reported CH_4 elimination as a minor channel in the metastable spectrum of $\text{HSi}^+(\text{CH}_3)_2$ ion [31], but their spectrum also shows a low-intensity product corresponding to loss of CH_3 and another because of loss of H_2 and H . These products suggest that the metastable $\text{HSi}^+(\text{CH}_3)_2$ ions have more internal energy in their instrument, such that higher-energy radical losses are possible. Based on our observations, we conclude that the CH_4 product we observe for the trimethylsilyl-substituted silylenium ions does not arise solely from the charged silicon center, but also derives either H or CH_3 from

the trimethylsilyl substituent, and consider now a mechanism for this reaction.

The peak shape for loss of methane was analyzed for four of the five ions. (Inadequate signal precluded the characterization of methane loss for the acetylene-bridged ion.) The KERDs for methane elimination are similar in shape to that observed for $(\text{CH}_3)_3\text{Si-Si}^+(\text{CH}_3)_2$, but show some small variation in the average energy released (Fig. 5). This suggests that the mechanisms are similar in all four ions in that they all involve significant reverse activation barriers, but that the barriers to elimination may vary. In contrast to the present results, Tobita et al. reported far greater variation in the KER for the $X = \text{O}$ and NH systems ($T_{0.5} = 482$ and 944 meV, respectively) [18]. The reason for this disagreement is not clear, but again

Table 4

Reaction enthalpy at 0 K for the elimination of C_2H_4 from $(\text{CH}_3)_3\text{Si-Si}^+(\text{CH}_3)_2$ and $(\text{CH}_3)_3\text{Si-X-Si}^+(\text{CH}_3)_2$ ($X = \text{CH}_2, \text{O}, \text{C}\equiv\text{C}$)^a

Reactant ion	Product ion (assumed)	HF/6-31G(d,p)	Becke3LYP/6-31G(d)
$(\text{CH}_3)_3\text{Si-Si}^+(\text{CH}_3)_2$	$(\text{CH}_3)_3\text{Si-Si}^+\text{H}_2$	2.25	2.49
$(\text{CH}_3)_3\text{Si-CH}_2\text{-Si}^+(\text{CH}_3)_2$	$(\text{CH}_3)_3\text{Si-CH}_2\text{-Si}^+\text{H}_2$	2.37	2.52
$(\text{CH}_3)_3\text{Si-O-Si}^+(\text{CH}_3)_2$	$(\text{CH}_3)_3\text{Si-O-Si}^+\text{H}_2$	2.55	2.74
$(\text{CH}_3)_3\text{Si-C}\equiv\text{C-Si}^+(\text{CH}_3)_2$	$(\text{CH}_3)_3\text{Si-C}\equiv\text{C-Si}^+\text{H}_2$	2.49	2.65

^a Energy relative to the precursor ion, in units of eV, and corrected for zero-point vibrational energy.

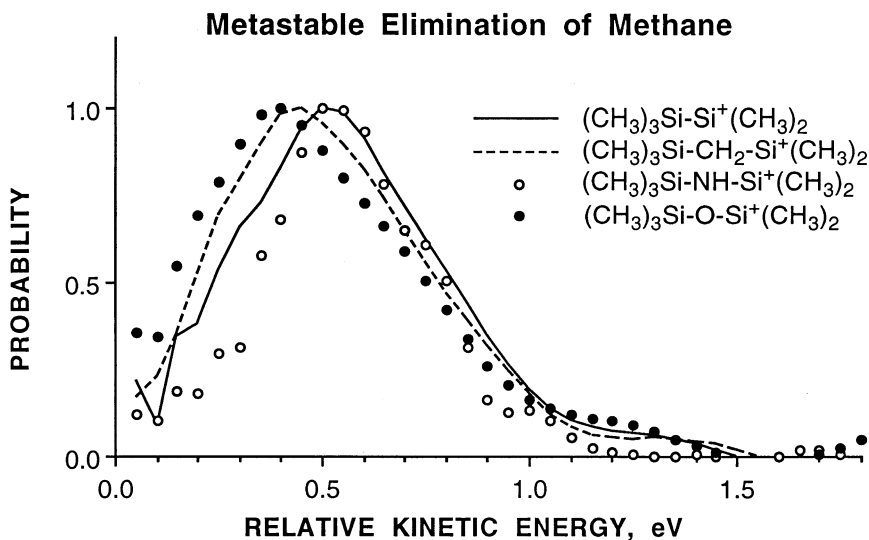


Fig. 5. Comparison of the experimental kinetic energy release distributions in $(\text{CH}_3)_3\text{Si-Si}^+(\text{CH}_3)_2$ and the $(\text{CH}_3)_3\text{Si-X-Si}^+(\text{CH}_3)_2$ series ($\text{X} = \text{CH}_2, \text{NH}, \text{O}$). Weak signal precluded measurement of the experimental distribution for $\text{X} = \text{C}\equiv\text{C}$.

may have to do with differences in the internal energies of the ions studied in the different instruments used.

As shown in Table 1, elimination of CH_4 is the dominant dissociation pathway for the $\text{X} = \text{CH}_2, \text{NH}$, and O ions. As in the case of $(\text{CH}_3)_3\text{Si-Si}^+(\text{CH}_3)_2$, this indicates that the barrier for the elimination of CH_4 must be significantly lower than that for C_2H_4 elimination for these ions, probably by about 0.8 eV (see Table 3). From the maxima of the KERDs for CH_4 elimination, an approximate value for the reverse activation barrier is 0.5 eV relative to the product

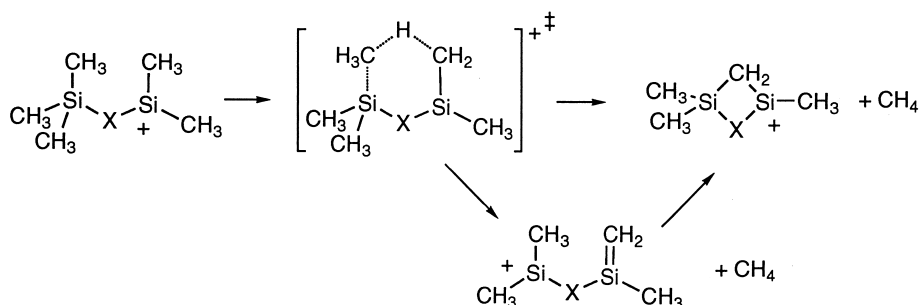
energies. The products formed by CH_4 elimination should therefore be about 1.3 eV more stable than the products formed by C_2H_4 elimination. This requirement places useful constraints on the range of possibilities for the structures of the ionic species. In Table 5 are shown the reaction enthalpies for formation of several alternative products from CH_4 loss for the $\text{X} = \text{O}$ precursor ion. Of these structures, the lowest energy 1,3-disilacyclobutyl cation is about 1.3–1.5 eV more stable than the ethylene loss product (Table 4), and all the other isomers considered are significantly higher in energy. This suggests that for this ion, as for

Table 5

Relative energies for some possible ionic products of elimination of CH_4 from $(\text{CH}_3)_3\text{Si-O-Si}^+(\text{CH}_3)_2^a$

Product Ion	HF/6-31G(d,p)	Becke3LYP/6-31G(d)
$(\text{CH}_3)_2\text{Si} \begin{array}{c} \diagup \\ \text{O} \\ \diagdown \end{array} \text{Si}^+\text{CH}_3$	1.27	1.10
$(\text{CH}_3)_2\text{Si-O} \begin{array}{c} \text{CH}_2 \\ \\ \text{SiCH}_3 \end{array}$	2.77	2.49
$(\text{CH}_3)_2\text{Si} \begin{array}{c} \diagup \\ \text{O}^+ \\ \diagdown \end{array} \text{Si}^+\text{CH}_3$	3.68	3.46
$(\text{CH}_3)_3\text{Si-O-Si}^+\text{CH}_2$	3.83	3.47

^a Energies are relative to the precursor ion, in units of eV and corrected for zero-point vibrational energy.



Scheme 3. Cyclic transition state for methane elimination.

$(\text{CH}_3)_3\text{Si}-\text{Si}^+(\text{CH}_3)_2$, methane elimination results in formation of a disilacyclobutyl cation.

Across the series of the ions studied, the branching ratio for CH_4 elimination is highly dependent on the bridging unit. For $\text{X} = \text{NH}$, O and CH_2 , methane elimination is by far the dominant reaction pathway. For $\text{X} = \text{C}\equiv\text{C}$ and for $(\text{CH}_3)_3\text{Si}-\text{Si}^+(\text{CH}_3)_2$ methane elimination becomes only a minor pathway (Table 1). We interpret these observations in terms of a cyclic transition state involving elimination across the two silicon centers (Scheme 3) in the unrearranged ions, and collapse of the resulting ion to the cyclic products. The inflexible $\text{C}\equiv\text{C}$ bridging unit introduces considerable strain to the transition state, effectively preventing CH_4 elimination. However, the five-membered ring that would be implicated for $(\text{CH}_3)_3\text{Si}-\text{Si}^+(\text{CH}_3)_2$ does not seem greatly strained by compar-

ison with a six-membered ring. For this ion, we propose an alternative mechanism, shown in Scheme 4. The rationale behind this proposal is as follows: Metastable dissociation of $(\text{CH}_3)_3\text{Si}-\text{Si}^+(\text{CH}_3)_2$ is unique in this series in that a major product formed corresponds to loss of H_2 . The phase space modeling suggests the transition state for this process is close in energy to that for CH_4 loss, and both processes are accompanied by large releases of kinetic energy, suggesting concerted eliminations. It seems plausible that a common intermediate is involved, one that is structurally analogous to the $\text{X} = \text{NH}$, O and CH_2 ions, but in which *either* H_2 or CH_4 elimination may occur by the six-membered ring transition state as in Scheme 3. This structure can be reached by means of an initial endothermic 1,2-hydrogen shift to form the β -silicon carbenium ion. The subsequent 1,2-

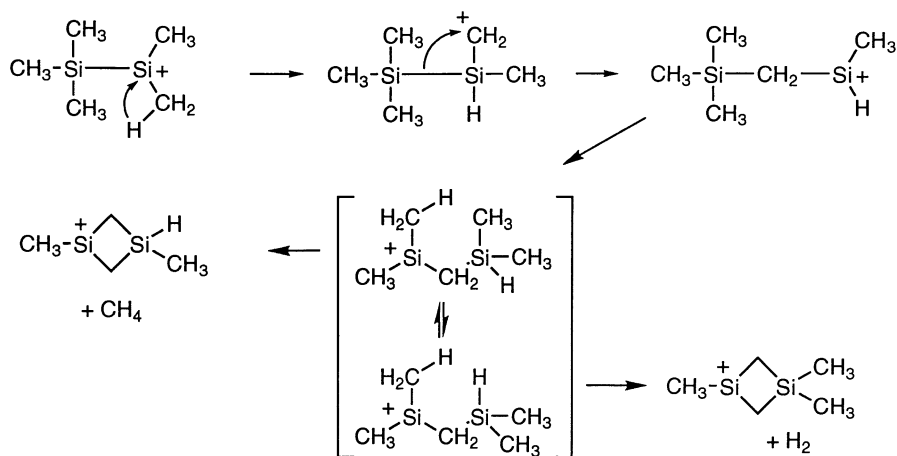
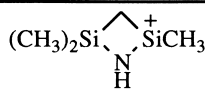
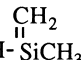
Scheme 4. Loss of H_2 or CH_4 from trimethylsilyldimethylsilylenium ion.

Table 6

Relative energies for some possible ionic products of elimination of CH₄ from (CH₃)₃Si–O–Si⁺(CH₃)₂^a

Product Ion	HF/6-31G(d,p)	Becke3LYP/6-31G(d)
	0.0	0.0
(CH ₃) ₂ Si ⁺ –N=Si(CH ₃) ₂	0.10	0.04
(CH ₃) ₂ Si ⁺ –NH– 	1.86	1.67
(CH ₃) ₃ Si–N=Si ⁺ CH ₃	2.37	2.00

^a Energies are relative to the cyclic structure, in units of eV, and corrected for zero-point vibrational energy.

Si(CH₃)₃ shift and 1,3-methyl shifts are both expected to be exothermic, and thus, lead to the proposed common intermediate species, and to elimination of H₂ or CH₄ by means of the cyclic transition state. This mechanism explains the unique H₂ loss channel in (CH₃)₃Si–Si⁺(CH₃)₂ by means of chemistry common to the other ions as well, and further provides a means to rearrange to the 1,3-disilacyclobutyl product species that are implicated by the phase space modeling.

The metastable loss of CH₄ from the (CH₃)₃Si–NH–Si⁺(CH₃)₂ ion is worthy of specific mention. Elimination of methane is nearly the exclusive dissociation pathway for this ion, with only a very small amount (<1%) of (CH₃)₃Si⁺ formation. Earlier deuterium labeling studies of this ion suggest that CH₄ loss involves the hydrogen on the bridging amino group [32]. Elimination across the Si–N bond would lead to the formation of either (CH₃)₂Si⁺–N=Si(CH₃)₂ or (CH₃)₃Si–N=Si⁺CH₃. The energies of these product ions, compared to the lowest-energy cyclic product, are shown in Table 6. The symmetric ion is quite stable and is comparable in energy to the cyclic structure formed by elimination across the two silicon centers. If the symmetric ion is in fact the product of methane elimination, the similarity of the KERD for elimination of methane from this ion to that for the other three ions would argue that the barriers for 1,2-methane elimination across the Si–N bond and for 1,4-elimination as shown in Scheme 3 are fortuitously similar in energy.

4. Conclusions

Metastable dissociations were studied for five trimethylsilyl-substituted silylenium ions: (CH₃)₃Si–Si⁺(CH₃)₂ and (CH₃)₃Si–X–Si⁺(CH₃)₂ (X = CH₂, NH, O, and C≡C). All of these ions except (CH₃)₃Si–NH–Si⁺(CH₃)₂ undergo elimination of C₂H₄, a process that has been observed previously in dimethyl-substituted silylenium ions, but this reaction is only a minor pathway. This reaction probably occurs by a stepwise mechanism analogous to that proposed for the HSi⁺(CH₃)₂ and (CH₃)₃Si⁺ species. A new dissociation is observed for the trimethylsilyl-substituted species as compared to other dimethyl-substituted silylenium ions, corresponding to loss of CH₄. This reaction involves a significant reverse activation barrier, and is strongly dependent on the nature of the bridging group, suggesting that the elimination is concerted and occurs across the two silicon centers.

Acknowledgements

This work was supported by a grant from NSF (CHE-9502038). We gratefully acknowledge the assistance of Tanya Kaminsky with some of the electronic structure calculations. STG also wishes to acknowledge Mike Bowers, who has been a valued teacher, mentor, and friend.

Appendix

The details of the calculations performed have been presented previously [17,24–27], so only particularly relevant points will be made here.

The vibrational frequencies and rotational constants used in the statistical phase space model for $(\text{CH}_3)_3\text{Si-Si}^+(\text{CH}_3)_2$ were obtained from ab initio calculations. For the product orbiting transition states, the frequencies and rotational constants for the separated ionic and neutral products were used. The vibrational frequencies and rotational constants for $(\text{CH}_3)_3\text{Si-SiH}_2^+$, $(\text{CH}_3)_3\text{Si}^+$ and $\text{Si}(\text{CH}_3)_2$ were taken from ab initio calculations while the parameters for C_2H_4 were taken from the literature [33]. The polarizability of $\text{Si}(\text{CH}_3)_2$ was estimated using additivity methods [34].

The potential energy surface model used for these calculations is shown in Fig. 2, and incorporates all four of the dissociation channels. On the basis of the large kinetic energy releases observed experimentally, tight transition states were assumed for elimination of H_2 and CH_4 . The frequencies for these transition states were estimated by starting with the calculated frequencies for the respective ionic products and adding an appropriate number of C–H stretch, Si–H stretch, methyl or methylene bend, and torsional frequencies. The experimental KERDs for the $(\text{CH}_3)_3\text{Si}^+$ channel suggests there is no reverse activation barrier, so an orbiting transition state [26] was used. Likewise, an orbiting transition state was used in the C_2H_4 loss channel.

The theoretical KERDs are calculated by determining the partitioning of energy between kinetic and internal for single values of total energy and total angular momentum, and then integrating over the energy and angular momentum distributions appropriate for the reactant ions. In both models, the timescale of the experiment was included, as has been described previously [17]. Internal energy distributions for the dissociating species are unknown, but use of several different test distributions showed no dependence of the resulting calculated KERD on the internal energy distribution assumed. This is a consequence of the

constraint of the experimental time window, which selects for a narrow energy range of ions.

References

- [1] T.M. Mayer, F.W. Lampe, *J. Phys. Chem.* 78 (1974) 2433.
- [2] W.N. Allen, F.W. Lampe, *J. Am. Chem. Soc.* 99 (1977) 6816.
- [3] R.N. Abernathy, F.W. Lampe, *J. Am. Chem. Soc.* 103 (1981) 2573.
- [4] C.H. DePuy, R. Damrauer, J.H. Bowie, J.C. Sheldon, *Acc. Chem. Res.* 20 (1987) 127.
- [5] H. Schwarz, in *The Chemistry of Organic Silicon Compounds*, S. Patai, Z. Rappoport (Eds.), Wiley New York, 1989, pp. 445–511.
- [6] T. Drewello, P.C. Burgers, W. Zummack, Y. Apeloig, H. Schwarz, *Organometallics* 9 (1990) 1161.
- [7] R. Bakhtiar, C.M. Holzngel, D.B. Jacobson, *J. Am. Chem. Soc.* 114 (1992) 3227.
- [8] D.A. Saulys, C.E.C.A. Hop, D.F. Gaines, *J. Am. Soc. Mass Spectrom.* 5 (1994) 537.
- [9] M.S. Gordon, L.A. Pederson, R. Bakhtiar, D.B. Jacobson, *J. Phys. Chem.* 99 (1995) 148.
- [10] A.E. Ketvirtus, D.K. Bohme, A.C. Hopkinson, *Organometallics* 14 (1995) 347.
- [11] S.G. Cho, *J. Organomet. Chem.* 510 (1996) 25.
- [12] I.S. Ignatyev, T. Sundius, *Organometallics* 15 (1996) 5674.
- [13] C.M. Holzngel, R. Bakhtiar, D.B. Jacobson, *J. Am. Soc. Mass Spectrom.* 2 (1991) 278.
- [14] R. Bakhtiar, C.M. Holzngel, D.B. Jacobson, *J. Phys. Chem.* 97 (1993) 12 710.
- [15] R. Bakhtiar, C.M. Holzngel, D.B. Jacobson, *Organometallics* 12 (1993) 880.
- [16] R. Bakhtiar, C.M. Holzngel, D.B. Jacobson, *Organometallics* 12 (1993) 621.
- [17] B.B. Willard, S.T. Graul, *J. Phys. Chem. A* 102 (1998) 6942.
- [18] S. Tobita, S. Tajima, F. Okada, S. Mori, E. Tabei, M. Umemura, *Org. Mass Spectrom.* 25 (1990) 39.
- [19] M.F. Jarrold, A.J. Illies, N.J. Kerchner, W. Wagner-Redeker, M.T. Bowers, M.L. Mandich, J.L. Beauchamp, *J. Phys. Chem.* 87 (1983) 2213.
- [20] B.A. Rumpf, P.J. Derrick, *Int. J. Mass Spectrom. Ion Processes* 82 (1988) 239.
- [21] M.J. Frisch, G.W. Trucks, M. Head-Gordon, P.M.W. Gill, M.W. Wong, J.B. Foresman, B.G. Johnson, H.B. Schlegel, M.A. Robb, E.S. Replogle, R. Gomperts, J.L. Andres, K. Raghavachari, J.S. Binkley, C. Gonzalez, R.L. Martin, D.J. Fox, D.J. Defrees, J. Baker, J.J.P. Stewart, J.A. Pople, Gaussian, Inc., Pittsburgh, PA, 1992.
- [22] M. J. Frisch, G.W. Trucks, H.B. Schlegel, P.M.W. Gill, B.G. Johnson, M.A. Robb, J.R. Cheeseman, T. Keith, G.A. Petersson, J.A. Montgomery, K. Raghavachari, M.A. Al-Laham, V.G. Zakrzewski, J.V. Ortiz, J.B. Foresman, J. Cioslowski, B.B. Stefanov, A. Nanayakkara, M. Challacombe, C.Y. Peng, P.Y. Ayala, W. Chen, M.W. Wong, J.L. Andres, E.S. Replogle, R. Gomperts, R.L. Martin, D.J. Fox, J.S. Binkley, D.J. Defrees, J.P. Baker, J.P. Stewart, M. Head-Gordon, C. Gonzalez, J.A. Pople, Gaussian, Inc.: Pittsburgh, PA, 1995.

- [23] W.J. Hehre, L. Radom, P.v.R. Schleyer, J.A. Pople, *Ab Initio Molecular Orbital Theory*, Wiley, New York, 1986.
- [24] W.J. Chesnavich, M.T. Bowers, *J. Am. Chem. Soc.* 98 (1976) 8301.
- [25] W.J. Chesnavich, M.T. Bowers, *J. Chem. Phys.* 68 (1978) 901.
- [26] W.J. Chesnavich, M.T. Bowers, In *Gas Phase Ion Chemistry*, M.T. Bowers (Ed.), Academic, New York, 1979, Vol. 1, pp. 119.
- [27] W.J. Chesnavich, M.T. Bowers, *Prog. React. Kin.* 11 (1982) 137.
- [28] R.E. Swaim, W.P. Weber, H.G. Boettger, M. Evans, F.M. Bockhoff, *Org. Mass Spectrom.* 15 (1980) 304.
- [29] K.R. Pope, P.R. Jones, *Organometallics* 3 (1984) 354.
- [30] M.A. Hanratty, J.L. Beauchamp, A.J. Illies, P. van Koppen, M.T. Bowers, *J. Am. Chem. Soc.* 110 (1988) 1.
- [31] E. Tabei, S. Mori, T. Kinoshita, K. Kawazoe, S. Tajima, *Rapid Comm. Mass Spectrom.* 7 (1993) 867.
- [32] J. Tamás, P. Miklós, *Org. Mass Spectrom.* 10 (1975) 859.
- [33] T. Shimanouchi, *Tables of Molecular Vibrational Frequencies, Consolidated Volume 1*; National Bureau of Standards, Washington, D. C., 1972.
- [34] K.J. Miller, J.A. Savchik, *J. Am. Chem. Soc.* 101 (1979) 7206.